Zebrafish *Hagoromo* Mutants Up-Regulate *fgf8* Postembryonically and Develop Neuroblastoma

Adam Amsterdam,[1] Kevin Lai,[1] Anna Z. Komisarczuk,[2] Thomas S. Becker,[2] Roderick T. Bronson,[3] Nancy Hopkins,[1] and Jacqueline A. Lees[1]

[1]*David H. Koch Institute for Integrative Cancer Research at MIT, Cambridge, Massachusetts,*
[2]*Sars Centre for Marine Molecular Biology, University of Bergen, Bergen, Norway, and*
[3]*Tufts Cummings School of Veterinary Medicine, North Grafton, Massachusetts*

Abstract

We screened an existing collection of zebrafish insertional mutants for cancer susceptibility by histologic examination of heterozygotes at 2 years of age. As most mutants had no altered cancer predisposition, this provided the first comprehensive description of spontaneous tumor spectrum and frequency in adult zebrafish. Moreover, the screen identified four lines, each carrying a different dominant mutant allele of *Hagoromo* previously linked to adult pigmentation defects, which develop tumors with high penetrance and that histologically resemble neuroblastoma. These tumors are clearly neural in origin, although they do not express catecholaminergic neuronal markers characteristic of human neuroblastoma. The zebrafish tumors result from inappropriate maintenance of a cell population within the cranial ganglia that are likely neural precursors. These neoplasias typically remain small but they can become highly aggressive, initially traveling along cranial nerves, and ultimately filling the head. The developmental origin of these tumors is highly reminiscent of human neuroblastoma. The four mutant *Hagoromo* alleles all contain viral insertions in the *fbxw4* gene, which encodes an F-box WD40 domain–containing protein. However, although one allele clearly reduced the levels of *fbxw4* mRNA, the other three insertions had no detectable effect on *fbw4* expression. Instead, we showed that all four mutations result in the postembryonic up-regulation of the neighboring gene, *fibroblast growth factor 8* (*fgf8*). Moreover, *fgf8* is highly expressed in the tumorigenic lesions. Although *fgf8* overexpression is known to be associated with breast and prostate cancer in mammals, this study provides the first evidence that *fgf8* misregulation can lead to neural tumors. (Mol Cancer Res 2009;7(6):841–50)

Introduction

The zebrafish is an increasingly popular model organism in which to study cancer (1). Mutation of known tumor suppressors such as *nf2, p53, apc*, and *mlh1* (2-5) result in cancer susceptibility, and tumorigenesis can also be driven by the expression of a number of oncogenes such as *c-myc* (6), mutant *Kras* (7), or mutant *braf* (8). Additionally, forward genetic screens in zebrafish can identify novel mutations that lead to cancer susceptibility. For example, by screening initially for mutations that affect the cell cycle in homozygous embryos, mutations in *bmyb* and *separase* were found to modestly increase the rate of carcinogen-induced cancer in heterozygous adults (9, 10). In another study, by conducting a pilot screen of an existing collection of heterozygous carriers of embryonic lethal insertional mutations for the development of externally visible spontaneous tumors, we established that the haploinsufficiency of 17 different ribosomal protein genes is highly tumorigenic (2, 11). This validates the use of zebrafish to identify novel cancer genes.

The mutant collection used for this pilot screen includes over 500 mutations in more than 370 genes (12). These mutations were made by retroviral insertion, allowing rapid identification of the mutated gene in almost all cases by cloning the genomic DNA flanking the mutagenic insertion (13). These mutants were recovered in a large-scale screen designed to find recessive mutations with embryonic phenotypes (14), and nearly all of the mutants are embryonic or larval lethal in their homozygous state. In the course of the screen, we also recovered a few dominant mutations with viable adult phenotypes affecting either pigmentation or fin growth. None of these dominant mutations had any visible phenotypes during embryogenesis as either heterozygotes or homozygotes.

We maintain all of the zebrafish mutant lines as stocks of 15 to 25 heterozygotes until 2 years of age, thereby allowing for an assessment of adult phenotypes in the heterozygous state. In this study, we extended our analysis of the full mutant collection by screening for spontaneous tumor development by histologic examination as opposed to just externally visible tumors. This revealed that all four alleles of the dominant mutation *Hagoromo* (14, 15) were highly predisposed to the development of neuroblastoma-like tumors arising in the cranial ganglia.

Received 12/4/08; revised 1/26/09; accepted 2/11/09; published OnlineFirst 6/16/09.
Grant support: NIH-National Cancer Institute grant CA106416 (N. Hopkins and J.A. Lees). The Sars Centre, the National Programme in Functional Genomics in Norway, and the European Commission as part of the ZF-Models Integrated Project in the 6th Framework Programme contract no. LSHG-CT-2003-503496 (T.S. Becker). J.A. Lees is a Ludwig Scholar at MIT.
The costs of publication of this article were defrayed in part by the payment of page charges. This article must therefore be hereby marked *advertisement* in accordance with 18 U.S.C. Section 1734 solely to indicate this fact.
Note: Supplementary data for this article are available at Molecular Cancer Research Online (http://mcr.aacrjournals.org/).
Current address for T.S. Becker: Brain and Mind Research Institute, University of Sydney, Camperdown, New South Wales 2050, Australia.
Requests for reprints: Jacqueline A. Lees, Koch Institute of Integrative Cancer Research, MIT Building E17-517B, Cambridge MA 02139. Phone: 617-252-1972; Fax: 617-253-9863. E-mail: jalees@mit.edu

doi:10.1158/1541-7786.MCR-08-0555

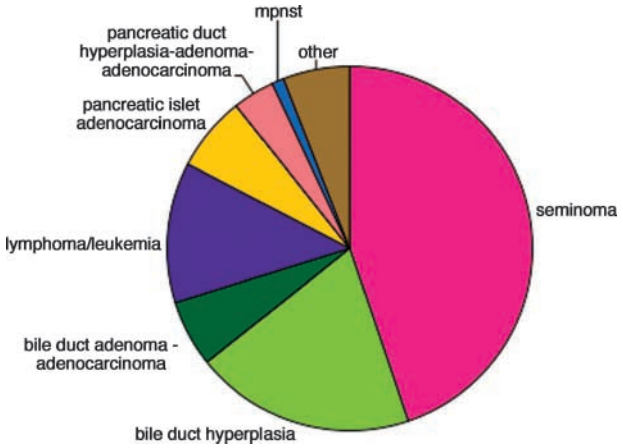

FIGURE 1. Distribution of types of tumorigenic lesions in the background population; data represents 473 cases of cancer or hyperplasia found amongst 9,988 2 yr old fish.

Results

Cancer Screen of Insertional Mutants Identifies Hagoromo

We had previously discovered that heterozygous mutation of many ribosomal protein (*rp*) genes, as well as the *nf2a* gene (one of two paralogs of the mammalian tumor suppressor *NF2*) predisposed zebrafish to the development of cancer, primarily malignant peripheral nerve sheath tumors (2). Notably, these mutants developed tumors spontaneously, in the absence of chemical carcinogens. Whereas the ribosomal protein mutants generally developed large, externally visible tumors, the *nf2a* heterozygotes usually developed much smaller tumors that were only evident upon histologic examination of the fish. Thus, it is unlikely that we would have discovered that these fish were tumor-prone had we not examined sections of a cohort of apparently healthy fish. Reasoning that there might be other mutations which similarly predisposed fish to tumors that might not be externally visible, we set about systematically examining heterozygotes from all of the insertional mutant lines in our collection by histology. Initially, we examined at least 15 fish for each line at ~2 years of age. In most cases, two longitudinal sections near either side of the midline were examined, although in some cases, six sections were screened. For any families that had a tumor frequency in the first cohort greater than background (see below), we collected additional 2-year-old fish to determine if this was a true tumor predisposition or just a sampling artifact.

All of the analyzed fish, with the exception of those from lines that we determined to be tumor-prone, served as a control set. Analysis of these 10,000 fish from 437 lines (including mutations in 341 different genes) indicated that the "background" frequency of tumorigenic lesions, including preadenoma bile duct hyperplasia, was ~5% at 2 years of age (473 of 9,988). The most common tumor types were seminomas and bile duct lesions (hyperplasia, adenoma, and adenocarcinoma), followed by pancreatic islet cell adenoma and leukemia/lymphoma (Fig. 1). None of these tumor types appeared in >2% of the fish and we did not find any families in which these tumors were significantly overrepresented. As far as we are aware, this is the first comprehensive analysis of spontaneous tumor incidence and spectrum in zebrafish.

Of the 342 loci screened in this manner, 339 were recessive embryonic lethal mutations. Beyond the previously noted *rp* and *nf2a* genes, none of the heterozygous carriers of recessive lethal mutations had a spontaneous cancer frequency significantly above background. This included mutations in two genes, *c-myb* and *separase*, in which heterozygous mutation has been shown to increase cancer frequency in carcinogen-treated fish (9, 10). In addition to these recessive mutations, the collection contains dominant mutations in three loci that have no embryonic phenotype (as homozygotes or heterozygotes) but rather have viable visible adult phenotypes either in fin growth or stripe patterning. One of these loci, for which we have four mutant alleles, is *Hagoromo* (*Hag*). *Hag* mutants, named for "the dress of a goddess", are characterized by disorganized stripes in the adult pigment pattern that are first apparent during the reorganization of iridophores and melanophores during metamorphosis at 3 to 4 weeks of age (15). Neither heterozygotes nor homozygotes have any embryonic phenotype; homozygotes are viable and have, on average, more severe stripe defects than heterozygotes, sometimes resulting in a spotty appearance in the anterior flank. All four *Hag* alleles carry insertions in the *fbxw4* gene, which encodes an F-box containing the WD40 repeat protein (15). Our screen revealed a significant tumor predisposition in these four *Hag* alleles. In each of these lines, 25% to 50% of 2-year-old heterozygotes had tumors that histologically resembled neuroblastoma (Table 1; Fig. 2). Importantly, these neuroblastoma-like tumors were not observed in any of the ~10,000 screened fish that lacked insertions in the *fbxw4* gene, including 150 noncarrier siblings from the *Hag* families. Thus, we conclude that fish without insertions in the *Hag* locus spontaneously develop this tumor type with a frequency of <1 in 10,000. This, coupled with the observation that four different insertions in this locus lead to this tumor type, indicates that the insertions at the *Hag* locus are unquestionably responsible for these cancers.

Hagoromo *Tumors Resemble Neuroblastoma and Are Preceded by the Inappropriate Maintenance of a Putative Neural Precursor Cell Population*

To better understand the nature and origin of these tumors, we conducted a careful analysis of the *Hag* fish. H&E staining

Table 1. Incidence of Neuroblastoma in 2-y-Old *Hag* Heterozygotes and their Wild-Type Siblings

Allele		Wild-type	Heterozygote (%)
hiD1	Total tumors	0/34	16/34 (47)
	Small neoplasias	0/34	7/34 (21)
	Advanced tumors	0/34	9/34 (26)
hiD2	Total tumors	0/56	19/77 (25)
	Small neoplasias	0/56	19/77 (25)
	Advanced tumors	0/56	0/77
hiD2058	Total tumors	0/39	17/38 (45)
	Small neoplasias	0/39	13/38 (34)
	Advanced tumors	0/39	4/38 (11)
hiD4000	Total tumors	0/24	18/59 (30)
	Small neoplasias	0/24	9/59 (15)
	Advanced tumors	0/24	9/59 (15)

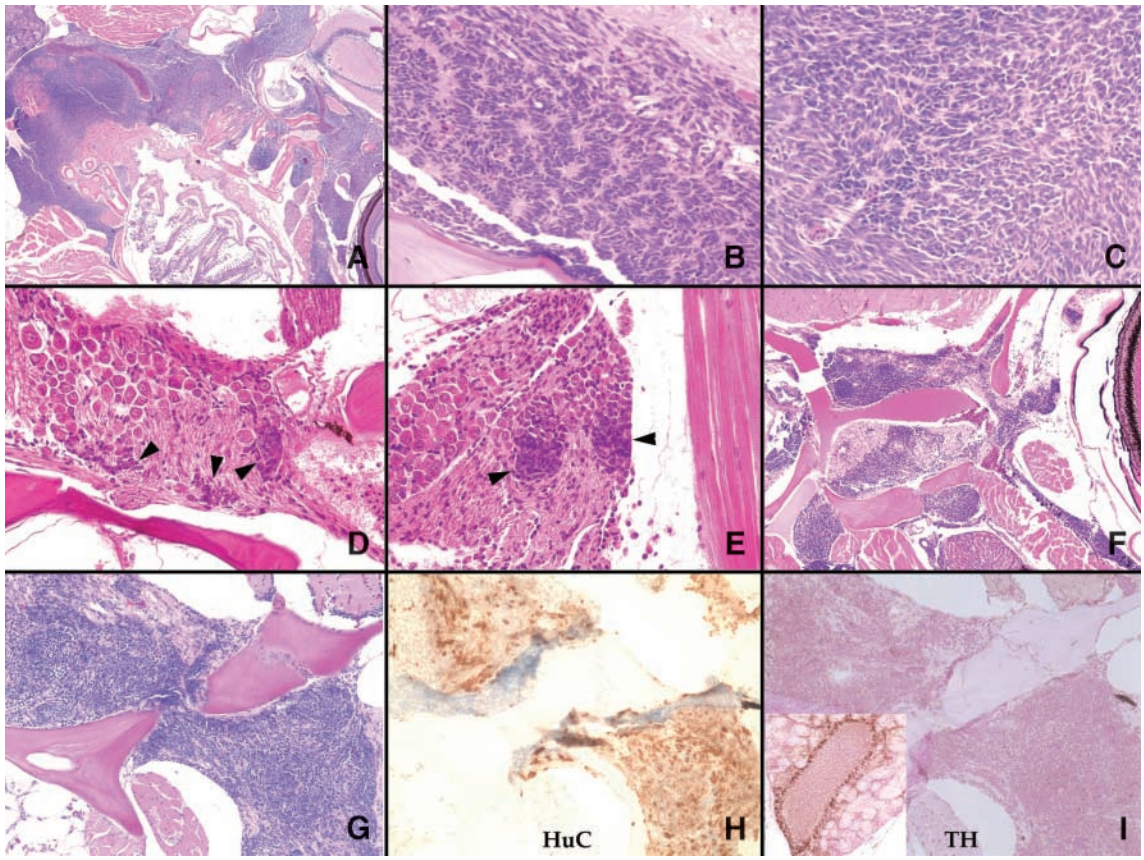

FIGURE 2. Neuroblastoma-like tumors in *Hag* heterozygotes at 2 y of age. **A.** A very advanced tumor fills most of the head space between the esophagus and the skull and invades the body wall musculature (original magnification, ×40). Rosette arrangement of cells is occasionally observed in tumors (**B**) but more commonly cellular arrangement is more variable (**C**; original magnification, ×400). Very small neoplasias (*black arrowheads*) observed in the ganglia within the skull below the midbrain (**D**) or posterior of the ear (**E**; original magnification, ×400). **F.** This tumor can be seen growing along the nerve running behind the eye as well as another below the skull (original magnification, ×100); H&E (**G**), anti-HuC (**H**), and anti-TH (**I**) of the same tumor (original magnification, ×200). Inset in **I**, TH staining of adrenal cells in the kidney on the same slide as a positive control for the antibody.

indicated that the tumors in *Hag* fish were made up of small, densely packed, oval cells with very little cytoplasm (Fig. 2). Although in some tumors, cells were arranged in "rosettes" (Fig. 2B) commonly seen in partly differentiated human neuroblastoma (16), more frequently, the cells were simply present as sheets with little organization (Fig. 2C), as is seen in undifferentiated human neuroblastoma (16). The tumors were found in a wide range of sizes, from small neoplasias (20-30 cells per planar section) to large tumors that occupied nearly the entire head, pushing aside (although never invading) the brain and pushing into the musculature of the cheeks and dorsal body wall. The highly aggressive tumors, such as that shown in Fig. 2A, were least common, and we rarely observed fish with any external signs of tumor growth, such as a bump on the dorsal surface or bulging of an eye. Small neoplasias were most common (Table 1) and always arose in cranial ganglia, either just below the midbrain but still within the skull (Fig. 2D), or in ganglia projecting posteriorly from behind the ear (Fig. 2E). As these tumors grew larger, they clearly overtook the entire ganglia and tracked along nerves, for example, those leaving the skull and projecting towards the ear or behind the eye (Fig. 2F). These tumors did not seem to be ganglioneuromas as they did not produce ganglion cells as they grew. Thus, based on the origin of these tumors in ganglia, as well as their histologic appearance, we suspected that they were neuroblastomas. By staining with the pan-neural marker HuC, we confirmed that these tumors were of neural origin (Fig. 2G and H). However, the tumors failed to stain for tyrosine hydroxylase (Fig. 2I). This marker is expressed in the catecholaminergic neurons of the peripheral sympathetic nervous system that are most often the cell of origin for human neuroblastoma (17, 18). Therefore, although these tumors were unquestionably neural and histologically resemble human neuroblastoma, they did not seem to arise from the same population of neurons that contributes to most human neuroblastoma. However, they may share other characteristics with the human disease.

Neuroblastoma is usually a neonatal or childhood cancer in humans. Tumors of this class typically originate from a precursor/progenitor population that persists inappropriately because of a failure to instigate the normal differentiation and/or apoptotic program (18, 19). In order to determine the origin of the tumors in *Hag* zebrafish, we conducted a time course analysis of the progeny of *Hag* heterozygous crosses (including wild-type, heterozygous, and homozygous sibs) by analyzing a

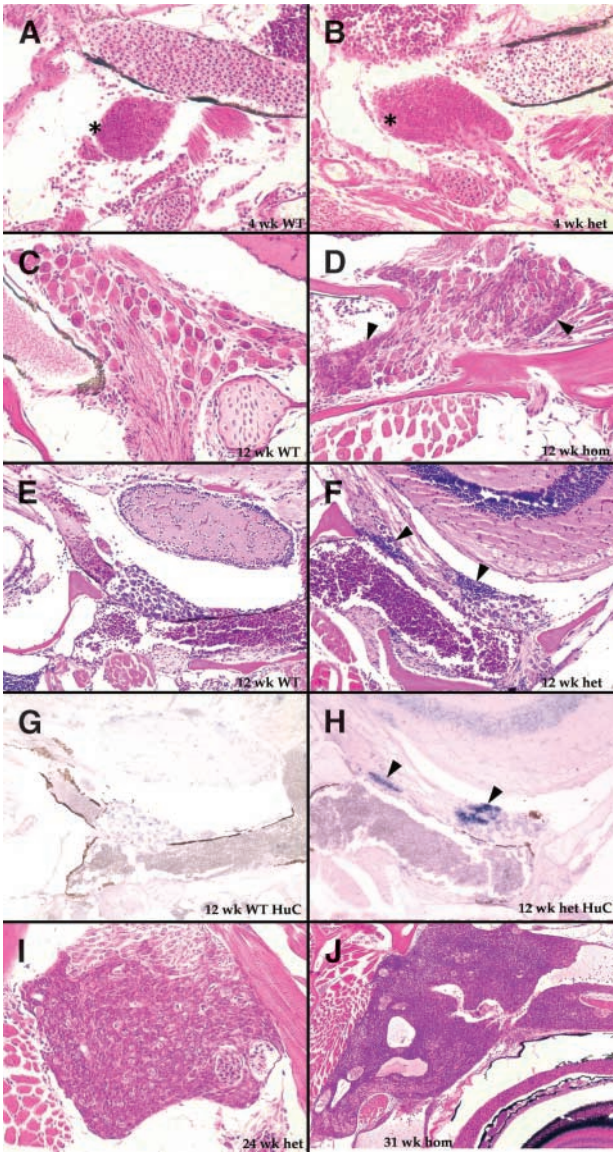

FIGURE 3. Tumors begin as inappropriate maintenance of a normal developmental stage of putative neural precursors. At 4 wk, small cells resembling the tumor cells (*asterisks*) are seen in cranial ganglia of both wild-type (**A**) and *Hag* (**B**) fish (original magnification, ×400); at 12 wk, only fully developed ganglion cells are observed in wild-type fish (**C**), but the small precursor-like cells (*black arrowheads*) are still observed in most *Hag* mutants (**D**; original magnification, ×400). **E-H.** The small cells seen uniquely in *Hag* mutants (*black arrowheads*) at 12 wk (**F**) stain strongly for HuC mRNA by *in situ* hybridization (**H**; original magnification, ×200); ganglion cells in wild-type (**E**) and *Hag* mutants (**F**) stain weakly for HuC (**G** and **H**); **I.** Tumor beginning to spread over the entire ganglia in 24-wk-old *Hag* heterozygote (original magnification, ×400); **J.** Tumor in 31-wk-old homozygote growing within the skull and along nerves behind and above the eye (original magnification, ×100).

subset of each cohort at 1-month intervals. The cranial ganglia of 1-month-old fish contained clusters of cells that appeared very similar in size, shape, and organization to the tumor cells (Fig. 3A and B). These were found in both wild-type and mutant fish, and thus we concluded that this is a normal developmental stage. However, by 2 months of age, these cells appeared less frequently and were fewer in number in wild-type fish than in either heterozygous or homozygous *Hag* fish (data not shown). This was even more apparent at 3 months, by which time these cells were completely absent in the wild-type fish, but they were maintained within almost all of the heterozygous and homozygous *Hag* mutants (Fig. 3C and D; Table 2). These cells were neural as they strongly express HuC (Fig. 3E-H). Taken together, these data suggest that the presence of this cell population in the wild-type zebrafish denotes a stage of neuronal development that is normally completed before 3 months of age. The simplest explanation for this finding is that these cells represent a neural precursor population. We believe that the persistence of these cells in 3-month-old *Hag* mutants is an early event in the tumorigenic process. Notably, these small neoplasias occurred at a similar frequency in both heterozygous and homozygous *Hag* mutants.

By as early as 5 months, these neoplasias began to grow into advanced tumors in a small proportion of *Hag* fish, spreading throughout entire ganglia and following nerve bundles away from their site of origin (Fig. 3I and J). These advanced tumors emerged at a slightly higher rate in homozygotes than in heterozygotes (Table 2). However, our ability to track tumor development in homozygotes was compromised by an additional phenotype of the homozygous fish; with variable penetrance, they developed severe inflammation in the wall of the posterior esophagus and anterior gut, leading to wasting and eventual mortality, possibly due to starvation (Table 2; Fig. S1). Taken as a whole, this time course experiment indicates that heterozygotes and homozygotes have a similar propensity to inappropriately maintain this presumed precursor cell population, but these neoplasias develop into more advanced tumors at a somewhat faster rate in homozygous versus heterozygous *Hag* mutants.

Hag *Mutations Up-Regulate* fgf8 *Expression Rather Than Affect* fbxw4

We wished to determine how the *Hag* mutant alleles contribute to the tumorigenic state. The insertional mutants used in this screen were made with Moloney murine leukemia virus (MoMLV)–based vectors. In mammals, MoMLV insertions can cause either gene activation through enhancer activity of the viral long terminal repeats (LTR) or inactivation by disruption of splicing or coding sequences (20, 21). Most of the mutants we recovered in our screen were recessive (491 of 497), and we isolated only six dominant mutations that represent insertions in three different loci (12, 14). Molecular analysis shows that in all of the recessive mutations that we examined, expression of the gene in which the insertion lies is reduced or abrogated (11, 13, 22). In contrast, the cause of the dominant mutations is less clear; they could be loss-of-function alleles of haploinsufficient loci or gain-of-function alleles.

To understand why the *Hag* mutants are tumor-prone, we first examined if expression of the *fbxw4* gene was affected, as all of the insertions lie within this gene, *hiD2058* at the splice donor of the first exon and *hiD1, hiD2*, and *hiD4000* all in the fifth intron (Fig. 4A). We chose to analyze gene expression in homozygotes as this would facilitate the detection of gene expression changes in cis to the insertion, especially if the effect was down-regulation. We used real-time reverse transcriptase PCR (RT-PCR) on RNA isolated from whole fish.

We examined the expression of *fbxw4* in wild-type fish and homozygotes for three of the lines at two developmental stages: the end of embryogenesis (5 days) and after juvenile morphogenesis (6 weeks), when the pigment phenotype that is the defining characteristic of the *Hag* mutants is clearly visible (Fig. 4B). For *hiD2058*, the mutant with an insertion at the splice donor of the first exon, expression was reduced to ~1% of wild-type levels (Fig. 4B). Additional analysis indicated that this insertion interferes with the splicing of the message, using a cryptic splice site in the first exon upstream of the initiation codon (data not shown). Thus, for *hiD2058*, the level of *fbxw4* is greatly reduced and is also incapable of producing full-length protein, if any protein at all. However, for two of the lines with insertions in the fifth intron (*hiD1* and *hiD4000*), there was no change in level of fbxw4 mRNA at either of these time points (Fig. 4B). Because all of the alleles have the same phenotype (both pigment and tumor phenotypes) but at least two of the three alleles with insertions in the large intron did not affect *fbxw4* expression (expression in *hiD2* was not examined), it is unlikely that the loss of *fbxw4*, even in *hiD2058*, was responsible for any of the observed phenotypes.

The gene immediately upstream of *fbxw4* is *fgf8* (Fig. 4A), and this juxtaposition is conserved between fish and mammals. *Fgf8* is a common site for mouse mammary tumor virus insertions in murine mammary cancer, in which viral insertions lead to *fgf8* overexpression (23-25). There are even some reported cases in which mouse mammary tumor virus had inserted in the murine *fbxw4* gene to cause activation of *fgf8* (25). Although we have not previously seen the MoMLV virus activate genes in zebrafish, given the mouse results, we thought it would be prudent to examine the effects of these insertions on *fgf8* expression in a manner identical to that used for *fbxw4*. During embryogenesis, *fgf8* expression is very dynamic and its function is especially important, as both loss-of-function mutants and mutations that lead to *fgf8* overexpression have early embryonic phenotypes (26, 27). In wild-type fish, *fgf8* expression declines after embryogenesis (Fig. 4C), although it is known to remain expressed in some tissues (28, 29). During embryogenesis, we did not see any differences in *fgf8* mRNA levels between whole wild-type fish and *Hag* homozygotes (Fig. 4C). However, at 6 weeks of age, *fgf8* mRNA levels were 6 to 12 times higher in *Hag* homozygotes than in wild-type controls for all three lines tested (Fig. 4B). To further explore this deregulation, we examined *fgf8* mRNA levels in wild-type and homozygous fish over a number of intervening time points for one allele (*hiD4000*; Fig. 4C). In wild-type fish, the overall level of *fgf8* mRNA began to decline 1 to 2 weeks after embryogenesis was complete, and *fgf8* mRNA dropped to very low levels by 5 to 6 weeks of age. In contrast, the amount of *fgf8* mRNA was maintained at near-embryonic levels in *Hag* homozygotes throughout the time course. Notably, there was an excellent correlation between the loss or maintenance of

Table 2. Incidence of Neural Neoplasias and Advanced Neuroblastoma in *Hag* Heterozygotes, Homozygotes, and Wild-type Siblings Over Time

Allele	Age (wk)		Wild-type	Heterozygotes (%)	Homozygotes (%)
hiD4000	12	Small neoplasias	0/17	28/30 (93)	17/20 (85)
		Advanced tumors	0/17	0/30	0/20
		Dead*	0/17	0/30	0/20
	24	Small neoplasias	0/10	20/28 (71)	7/9 (78)
		Advanced tumors	0/10	1/28 (4)	0/9
		Dead*	0/10	0/28	4/13 (31)
	31	Small neoplasias	0/16	18/28 (64)	0/2
		Advanced tumors	0/16	0/28	1/2 (50)
		Dead*	0/16	0/28	6/8 (75)
	39	Small neoplasias	N.D.	6/14 (43)	3/10 (30)
		Advanced tumors	N.D.	2/14 (14)	4/10 (40)
		Dead*	N.D.	0/14	7/17 (41)
hiD1	17	Small neoplasias	0/10	22/26 (85)	9/11 (82)
		Advanced tumors	0/10	0/26	0/11
		Dead*	N.D.	N.D.	N.D.
	24	Small neoplasias	0/21	37/52 (71)	3/13 (38)
		Advanced tumors	0/21	6/52 (11)	4/13 (31)
		Dead*	N.D.	N.D.	N.D.
	34	Small neoplasias	N.D.	3/10 (30)	3/7 (43)
		Advanced tumors	N.D.	3/10 (30)	2/7 (29)
		Dead*	N.D.	0/10	2/7 (29)
hiD2058	17	Small neoplasias	0/16	14/17 (82)	9/11 (82)
		Advanced tumors	0/16	0/17	0/11
		Dead*	N.D.	N.D.	N.D.
	24	Small neoplasias	0/15	29/37 (78)	8/11 (73)
		Advanced tumors	0/15	0/37	2/11 (18)
		Dead*	N.D.	N.D.	N.D.
	34	Small neoplasias	0/6	5/11 (45)	4/14 (29)
		Advanced tumors	0/6	4/11 (36)	6/14 (43)
		Dead*	0/6	0/11	4/18 (22)
hiD2	24	Small neoplasias	0/12	33/38 (87)	11/17 (64)
		Advanced tumors	0/12	0/38	1/17 (6)
		Dead*	N.D.	N.D.	N.D.

Abbreviation: N.D., not determined.
*These fish died from wasting, presumably subsequent to severe esophageal/gut inflammation, not from tumors.

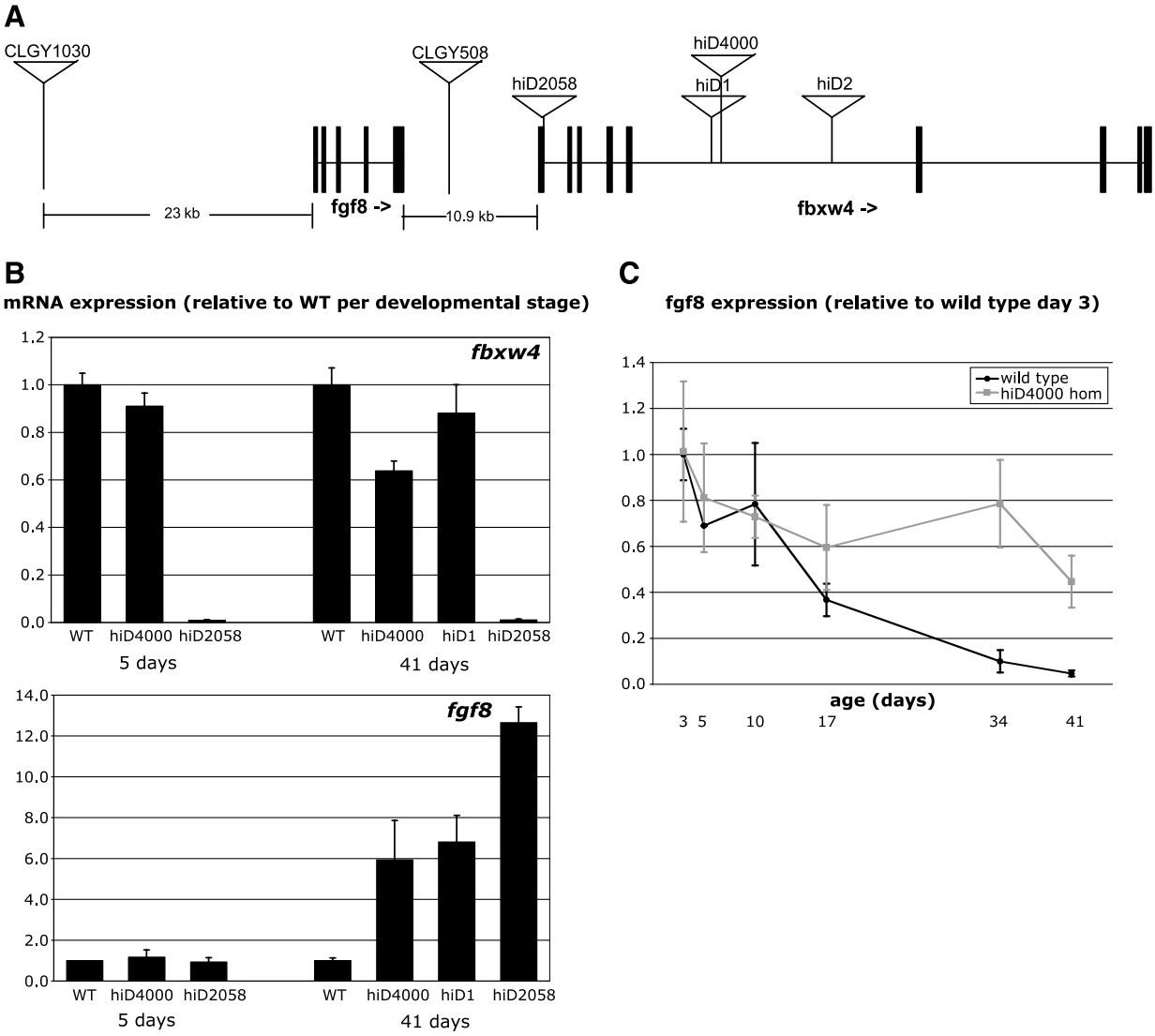

FIGURE 4. *Hag* mutations are insertions in the *fbxw4* gene but affect the expression of the neighboring *fgf8* gene. **A.** Location of the mutagenic insertions in *Hag* mutants. *hiD2058* is precisely at the splice donor of exon 1 of *fbxw4*; the other three insertions are in the 24 kb fifth intron. Enhancer trap insertions CLGY1030 and CLGY508 are in intergenic sequences upstream and downstream of *fgf8*, respectively. **B.** *fbxw4* and *fgf8* mRNA measured in whole fish by real-time RT-PCR in wild-type and homozygotes of multiple *Hag* alleles at 5 and 41 d. Units are normalized to wild-type sample of each developmental age (*columns,* mean of two to three technical replicates; *bars,* SD). **C.** *fgf8* mRNA measured in whole fish by real-time RT-PCR in wild-type and *hiD4000* homozygotes from 3 to 41 d. Units are normalized to the 3-d wild-type sample (*points,* mean of two to three technical replicates; *bars,* SD).

fgf8 mRNA in the wild-type and *Hag* mutant fish and the loss or maintenance of the presumed neural precursor population. Importantly, the timeframe of *fgf8* down-regulation precedes the loss of putative precursor cells in wild-type fish, suggesting that high *fgf8* somehow contributes to the maintenance of this population in the *Hag* mutants. As expression was measured from RNA prepared from whole fish, it is not clear if this difference is the result of higher levels of *fgf8* in cells that normally express it or ectopic expression of *fgf8*. Nonetheless, it is clear that *fgf8* is dramatically up-regulated in *Hag* mutants and that it is likely *fgf8*, not *fbxw4*, which is the gene responsible for the *Hagoromo* phenotypes. Consistent with this hypothesis, we note that an enhancer trap screen using another MoMLV-based retrovirus (30) yielded two insertions, CLGY1030 and CLGY508 (31), which lie in intergenic sequences upstream and downstream of *fgf8*, respectively (Fig. 4A). Analysis of *fgf8* expression in these mutants revealed both increased *fgf8* expression in the midbrain-hindbrain boundary at 3 day old and ectopic *fgf8* expression in the spinal region of 35 day old fish, and these two mutants develop a striped phenotype that is highly reminiscent of our *Hagoromo* mutants.[4] Histologic ana-lysis of these lines show that they also develop neuroblastoma tumors (Fig. S2). Taken together, these data strongly suggest that the tumor predisposition in these six lines result from a failure to down-regulate *fgf8* subsequent to embryogen-

[4] A. Komisarczuk and T.S. Becker, unpublished data.

esis and the consequent persistence of a putative neuronal precursor population.

As a further test of this hypothesis, we wished to determine if increased *fgf8* expression occurs in the region of the cranial ganglia from which the tumors originate. Thus, we analyzed *fgf8* expression by both semiquantitative RT-PCR and real-time RT-PCR on mRNA from several parts of the head of wild-type and both heterozygous and homozygous *Hag* fish at 3 months of age, the time at which the clusters of neural precursors are first completely absent in wild-type fish but maintained in the *Hag* mutants. The tissues analyzed included the brain, the skull, the soft tissue ventral to the skull (which included the cranial ganglia), and the jaws and skin. Of these tissues, the brain had the highest overall *fgf8* expression in wild-type fish, and *fgf8* expression seemed slightly higher in the brain of *Hag* mutants. The other three tissues, in which *fgf8* was expressed at a low level in wild-type fish, showed dramatically higher levels of *fgf8* in *Hag* mutants (Fig. 5A). Thus, we conclude that elevated *fgf8* expression is not restricted to the cranial ganglia but is clearly present in this region of the *Hag* mutants. Most importantly, *in situ* hybridization with antisense *fgf8* probe on sections cut from fish with tumors shows robust expression of *fgf8* in most, although not all, cells in the tumor (Fig. 5B and C). Thus, we conclude that the neuroblastomas themselves express *fgf8* at a very high level.

Discussion

Through the unbiased histologic screening of a collection of zebrafish insertional mutants, we determined that four independent lines carrying mutations in the *Hagoromo* locus develop neuroblastoma-like tumors at high penetrance. In some regards, these tumors are quite different from human neuroblastoma, which arises from neural crest–derived neural precursors in the sympathetic nervous system and grow predominantly in the abdomen or neck (17, 18). Tumors in *Hagoromo* fish arise in cranial ganglia and grow in the head. Although they are clearly of neural origin, as judged by their expression of

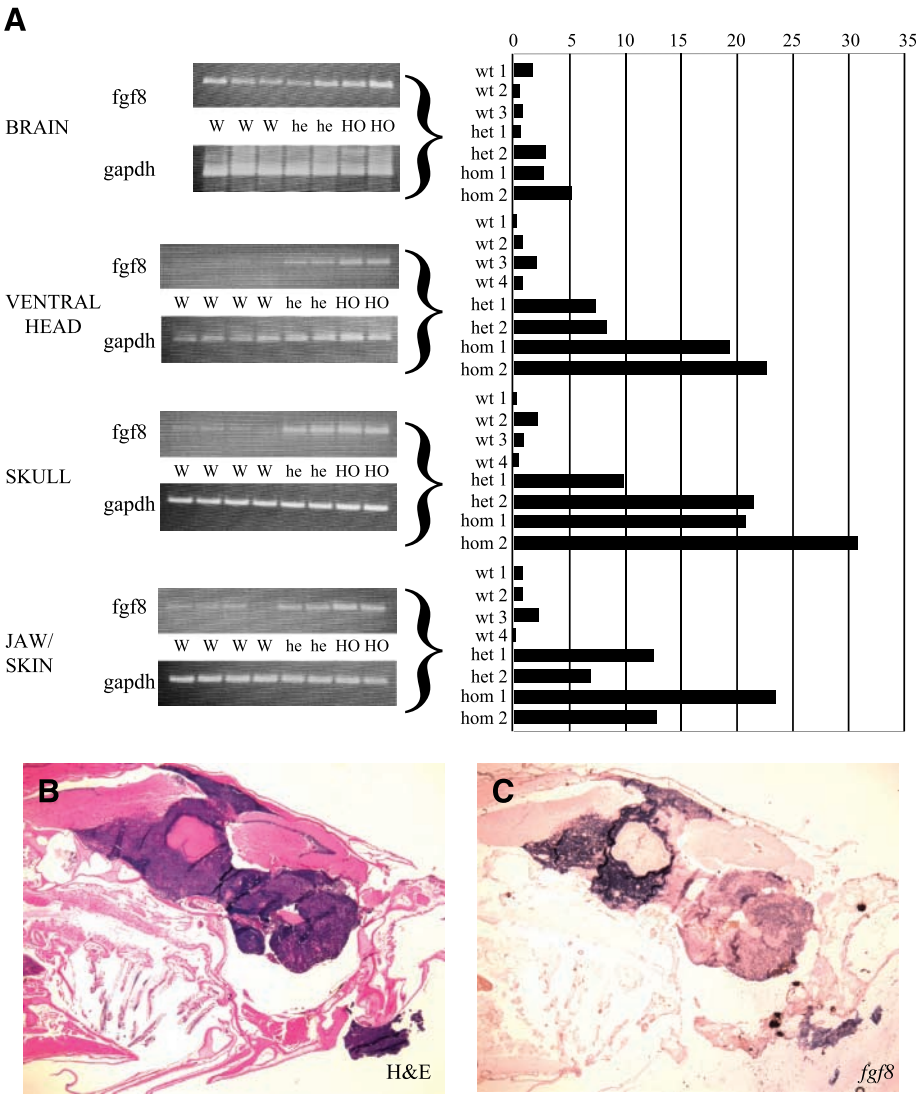

FIGURE 5. *Hag* mutants overexpress *fgf8* in the head region of young adults and in tumors. **A.** *fgf8* mRNA in multiple parts of the head of 3-mo-old wild-type, *hiD2058* heterozygote and *hiD2058* homozygote fish were measured by real-time and semiquantitative RT-PCR; *gapdh* was used as a normalization control. Samples were isolated from three (brain) or four wild-type fish and two each of Hag^{hi2058} heterozygotes and homozygotes. Ethidium bromide–stained gels from semiquantitative RT-PCR (*left*); quantification of real-time PCR (*right*). Quantification is normalized within the data set for each tissue to the average wild-type sample of that tissue; error bars show the SD of three technical replicates. **B** and **C.** (original magnification, ×20) H&E (**B**) and *fgf8 in situ* hybridization (**C**) on a very advanced tumor in a 2-y-old *hiD2058* homozygote.

HuC, these zebrafish tumors do not express markers of catecholaminergic neurons, indicating that they are derived from a different neural lineage than human neuroblastoma. Despite this difference, the *Hagoromo* tumors seem to arise through a similar mechanism as the human disease. Specifically, human neuroblastoma typically arises in infants and is thought to be a tumor of embryonic origin, i.e., derived from neural precursors present during fetal development (18, 19). Our analysis shows that wild-type zebrafish have a population of cells which exists in the cranial ganglia of juvenile fish but is lost as the fish grow to adulthood. We hypothesize that these cells represent neural precursors, and their disappearance, presumably through differentiation or apoptosis, reflects the normal developmental program. These cells are inappropriately maintained in *Hagoromo* mutants and they are the originating cell of the *Hagoromo* mutant tumors. Although in many cases, these clusters of cells fail to grow past the size of small neoplasias, in 10% to 20% of the mutants, they eventually grow into advanced tumors beginning as early as 5 months. This stochastic event likely reflects the need to acquire additional mutations within these cells. The *Hagoromo* mutation seems to act by prolonging the existence, and possibly driving the expansion, of this target cell population.

The four *Hagoromo* mutant lines each carry viral insertions in the *fbxw4* gene. However, our data show that they do not have a shared effect on *fbxw4* expression: one allele, in which the insertion lies at the splice donor of the first exon, diminished *fbxw4* mRNA levels, but the other insertions, which lie in the fifth intron, had no detectable effect on *fbxw4*. Instead, our data suggests that the key consequence of the *Hagoromo* insertions is to maintain high levels of *fgf8* expression after embryogenesis. Specifically, we find that *fgf8* mRNA is dramatically up-regulated in *Hagoromo* mutants after the completion of embryonic development, including expression in the head region where the inappropriately maintained precursors are first observed. In addition, very high *fgf8* expression is seen in the tumors themselves. Finally, insertional mutants have been recovered with a related virus from a different screen with phenotypes including both the stripe phenotype and the neuroblastoma phenotype in which the insertions lie outside of *fbxw4*, either between *fgf8* and *fbxw4* or upstream of *fgf8*, distal to *fbxw4*.

The mechanism by which these insertions activate *fgf8* expression is unclear. That the gene containing the viral insertions is not truly the affected gene should serve as a cautionary example for the analysis of other insertional mutants. In this case, although we cannot rule out direct viral activation, our previous studies suggest that the MoMLV LTR does not activate transcription in zebrafish cells; viruses relying on the LTR to drive the expression of the *lacZ* gene produced no β-galactosidase activity, whereas viruses with an internal promoter driving *lacZ* were able to do so (32). Additionally, in all other cases in which the expression of genes at the site of MoMLV insertions in zebrafish had been examined, gene expression had either decreased or was unaffected (11, 13, 22, 33). Thus, we instead favor the notion that the virus disrupts the transcriptional control of *fgf8* by distal *cis*-acting elements. This hypothesis is supported by several lines of evidence showing that *fgf8* expression is controlled by a number of enhancers upstream, within, and downstream of the gene, including elements within the *fbxw4* gene (31, 34, 35). Additionally, retroviral insertions in the *Fgf8/Fbxw4* locus in the mouse (36, 37) or genomic duplications near *FGF8* in humans (38, 39) cause a limb outgrowth phenotype (*dactylaplasia* or *split hand foot malformation*, respectively). The mechanism of these mouse and human mutations is not understood. However, the mouse mutants have been shown to have a defect in the maintenance of the apical ectodermal ridge of the developing limb, and *Fgf8* expression is normal at the beginning of limb development but is quickly lost (36). Although it has been suggested that this altered *Fgf8* expression is a secondary consequence of apical ectodermal ridge loss, it also seems possible that the insertions in the mouse *dactylaplasia* mutants affect *fgf8* expression in a direct, but complex, way that somehow accounts for the observed down-regulation after limb development begins. Although the molecular and phenotypic consequences of insertions and chromosomal rearrangements of the *Fgf8/Fbxw4* locus clearly differ between mammals and fish, it seems plausible that the resulting phenotypes in each organism (limb outgrowth defects in mammals, maintenance of neural precursor cells and stripe disruption in zebrafish) can be accounted for by differential effects on *fgf8* expression.

Regardless of the mechanism by which the zebrafish insertions cause continued high levels of *fgf8* expression after embryogenesis, it clearly leads to the inappropriate maintenance and expansion of a putative neural precursor population that ultimately become tumors. We note that the increase in *fgf8* expression in the head region of *Hagoromo* fish occurs at a time when this cell population diminishes in wild-type fish. This suggests that *fgf8* is capable of contributing to the maintenance of these cells, either by blocking differentiation or by promoting survival. It would seem paradoxical that *fgf8* should prevent the differentiation of these precursor cells as many studies have associated *fgf8* with neural differentiation. A requirement for *fgf8* in the development of neurons in various areas of both the central and peripheral nervous system, including the epibranchial placodes that give rise to the cranial ganglia, has been shown both in zebrafish (40-42) and in mice (43). Furthermore, *Fgf8* cooperates with retinoic acid to force mouse embryonic carcinoma P19 cells to differentiate into neurons, whereas inhibition of fgf signaling in this cell culture system attenuates neural differentiation (44). However, this prodifferentiation role for *fgf8* might be restricted to specific developmental stages such as embryogenesis. For example, in some settings, *fgf8* signaling can promote the proliferation of neural precursors at the expense of differentiation (45). The other possibility, that *fgf8* acts as a prosurvival signal for these cells, is supported by the observation that several fgfs, including *fgf8*, have antiapoptotic functions in both neural crest and ectoderm-derived neurons (43, 46). The effects of *fgf8* on differentiation and survival may depend on timing and context, such that early in development, neural differentiation is the favored response, but sustained *fgf8* expression past the time when such differentiation normally occurs may result in inappropriate survival and/or proliferation of the few remaining neural precursor cells.

Thus, *fgf8* seems to be an oncogene, in that its overexpression predisposes zebrafish to tumorigenesis. However, the tumor phenotype in *Hagoromo* mutants is not fully penetrant.

Notably, it seems that *fgf8* overexpression in *Hagoromo* mutants is always sufficient to disrupt the orderly alignment of pigment cells (which are moving into their stripe pattern at the time when we first see *fgf8* overexpression in the mutants), as well as the inappropriate maintenance of putative neural precursor cells in the cranial ganglia. However, these only progress to tumors in a subset of cases, suggesting that additional mutations are required. It is possible that there is only a limited window of opportunity for the precursor cell population to acquire these changes. This model is supported by our finding that small neoplasias exist in nearly all of the mutants at 3 to 6 months of age (and we might miss some due to sampling only three sections per fish) but are detected in fewer than half of the fish at 2 years of age. Thus, we speculate that *fgf8* overexpression allows for the persistence of a cell population that is then a target for additional mutations, and there may be a limited time in which such mutations can contribute to tumorigenesis. We do not currently know what these additional mutagenic events are, and this is an important question for future studies. However, we believe it is unlikely that mutation of the tumor suppressor gene *p53* is one such key event, as fish mutant for both *Hagoromo* and *p53* (3) do not have a higher rate of neuroblastoma formation by 1 year of age compared with fish mutant for *Hagoromo* alone (data not shown).

Fgf8 has also been implicated in tumorigenesis in other tumor types in mammals. Overexpression of *FGF8* has been observed in a number of human tumors, especially prostate and breast cancer (47-49). Furthermore, whole genome association studies indicate that specific polymorphisms in the fgf receptor *FGFR2* correlate with an increased frequency of breast cancer (50, 51). Direct evidence for the oncogenic properties of *Fgf8* in these tissues is even clearer in mice. The *Fgf8* locus is a common insertion site for mouse mammary tumor virus in retrovirus-induced mammary tumors (23-25), implying that its activation in mammary tissue can lead to tumorigenesis. Additionally, transgenic tissue-specific overexpression of *Fgf8* cooperates with *Pten* loss in mouse models of prostate cancer (52). Thus, *FGF8* seems to function as an oncogene in numerous settings, including prostate and breast cancer in mammals, and now neuroblastoma in zebrafish.

Materials and Methods

Fixation and Histology

Adult fish were euthanized in 500 mg/L tricaine and fixed in either Bouin's fixative or 10% neutral buffered formalin (in cases in which we wished to retain the option of immunohistochemistry or *in situ* hybridization). Embedding in paraffin and sectioning were done as previously described (2, 53). Prior to fixation, a piece of tail tissue was retained for the isolation of genomic DNA and either Southern analysis or PCR was conducted to determine the genotype of fish from the *Hag* heterozygous crosses (54).

Antibody Staining

Slides from fish fixed in 4% paraformaldehyde/PBS and paraffin embedded were stained as previously described (55). Primary antibodies used were anti-TH (1:100; Pel-Freez) and anti-HuC (1:250; Molecular Probes).

RNA Hybridization

Dig-labeled riboprobes were produced for both sense and antisense strands of the coding regions of the zebrafish *fgf8* and *HuC* genes using a dig-labeling kit (Roche) Slides from fish fixed in 4% paraformaldehyde/PBS and paraffin embedded were dewaxed (55), rinsed with PBS, treated with proteinase K (40 μg/mL) for 7 min, rinsed with PBS, refixed in 4% paraformaldehyde/PBS for 20 min, rinsed with PBS, and rinsed twice in 2× SSC. They were then prehybridized in hybridization solution (50% formamide, 5× SSC, 0.1% Tween, 1 mg/mL tRNA, and 50 μg/mL heparin) for 3 h at 70°C, and hybridized overnight at 70°C in a humid box with 100 μL of hybridization solution plus probe (1 μg/mL) under a coverslip. Slides were washed at 70°C for 10 min with 75% hyb/25% 2× SSC, 50% hyb/50% 2× SSC, 25% hyb/75% 2× SSC, 2× SSC, and for 30 min with 0.2× SSC. Slides were equilibrated in MAB + 0.1% Tween for 30 min, blocked in MAB + 0.1% Tween + 10% lamb serum + 2% blocking reagent (Roche), then alkaline-phospatase-conjugated anti-DIG Fab fragments were applied (1:1,000; Roche), overnight at 4°C. Antibody was washed five times for 30 min in MAB + 0.1% Tween, and alkaline phosphatase activity was detected with nitroblue tetrazolium/5-bromo-4-chloro-3-indolyl phosphate as recommended by the manufacturer (Roche). Figures show results with antisense probes; no blue stain was observed with sense strand probes of simultaneously processed adjacent level slides.

Quantitative RNA Analysis

RNA was prepared from embryos, adult fish tissues, or whole juvenile fish using Trizol reagent (Invitrogen); in the case of whole fish, 17 dpf or older, fish were flash-frozen in liquid nitrogen and mashed in a mortar and pestle prior to homogenization in Trizol. First-strand cDNA was prepared using Superscript III reverse transcriptase (Invitrogen) and gene expression levels were determined using real-time PCR with Sybr Green Master Mix (ABI). Standard curves were established for each primer set with cDNA dilutions and all samples were run in triplicate and normalized with primers for gapdh. All primer sequences are available upon request.

Disclosure of Potential Conflicts of Interest

No potential conflicts of interest were disclosed.

Acknowledgments

We thank Sarah Farrington and Kate Anderson for maintenance of the mutant lines of fish and assistance in sample collection; Tim Angelini and Sam Farrington for maintenance of the zebrafish colony; the Histology Facility of the MIT Koch Institute for Integrative Cancer Research, especially Alicia Caron and Weijia Zhang, for sample processing and sectioning; and Drs. A. Thomas Look and Jeffery Kutok for helpful discussions and consultation on histopathology.

References

1. Feitsma H, Cuppen E. Zebrafish as a cancer model. Mol Cancer Res 2008;6:685–94.

2. Amsterdam A, Sadler KC, Lai K, et al. Many ribosomal protein genes are cancer genes in zebrafish. PLoS Biol 2004;2:E139.

3. Berghmans S, et al. tp53 mutant zebrafish develop malignant peripheral nerve sheath tumors. Proc Natl Acad Sci U S A 2005;102:407–12.

4. Haramis AP, Hurlstone A, van der Velden Y, et al. Adenomatous polyposis coli-deficient zebrafish are susceptible to digestive tract neoplasia. EMBO Rep 2006;7:444–9.

5. Feitsma H, Kuiper RV, Korving J, Nijman IJ, Cuppen E. Zebrafish with mutations

in mismatch repair genes develop neurofibromas and other tumors. Cancer Res 2008;68:5059–66.

6. Langenau DM, Traver D, Ferrando AA, et al. Myc-induced T cell leukemia in transgenic zebrafish. Science 2003;299:887–90.

7. Langenau DM, Keefe MD, Storer NY, et al. Effects of RAS on the genesis of embryonal rhabdomyosarcoma. Genes Dev 2007;21:1382–95.

8. Patton EE, Widlund HR, Kutok JL, et al. BRAF mutations are sufficient to promote nevi formation and cooperate with p53 in the genesis of melanoma. Curr Biol 2005;15:249–54.

9. Shepard JL, Amatruda JF, Stern HM, et al. A zebrafish bmyb mutation causes genome instability and increased cancer susceptibility. Proc Natl Acad Sci U S A 2005;102:13194–9.

10. Shepard JL, Amatruda JF, Finkelstein D, et al. A mutation in separase causes genome instability and increased susceptibility to epithelial cancer. Genes Dev 2007;21:55–9.

11. Lai K, Amsterdam A, Farrington S, et al. Many ribosomal protein mutations are associated with growth impairment and tumor predisposition in zebrafish. Dev Dyn 2008;238:76–85.

12. Amsterdam A, Nissen RM, Sun Z, et al. Identification of 315 genes essential for early zebrafish development. Proc Natl Acad Sci U S A 2004;101:12792–7.

13. Gaiano N, Amsterdam A, Kawakami K, et al. Insertional mutagenesis and rapid cloning of essential genes in zebrafish. Nature 1996;383:829–32.

14. Amsterdam A, Burgess S, Golling G, et al. A large-scale insertional mutagenesis screen in zebrafish. Genes Dev 1999;13:2713–24.

15. Kawakami K, Amsterdam A, Shimoda N, et al. Proviral insertions in the zebrafish hagoromo gene, encoding an F-box/WD40-repeat protein, cause stripe pattern anomalies. Curr Biol 2000;10:463–6.

16. Machin GA. Histogenesis and histopathology of neuroblastoma. In: Pochedly C, editor. Neuroblastoma: clinical and biological manifestations. Elsevier Biomedical: New York; 1982, p. 195–231.

17. McConville CM, Forsyth J. Neuroblastoma—a developmental perspective. Cancer Lett 2003;197:3–9.

18. Brodeur GM, Maris JM. Neuroblastoma. In: Pizzo PA, Poplack DG, editors. Principles and practice of pediatric oncology. Lippincott Williams & Wilkins: Philadelphia; 2002, p. 895–937.

19. Dyer MA. Mouse models of childhood cancer of the nervous system. J Clin Pathol 2004;57:561–76.

20. Jaenisch R, Soriano P. Retroviruses as tools for mammalian development. Symp Fundam Cancer Res 1986;39:59–65.

21. Mikkers H, Berns A. Retroviral insertional mutagenesis: tagging cancer pathways. Adv Cancer Res 2003;88:53–99.

22. Golling G, Amsterdam A, Sun Z, et al. Insertional mutagenesis in zebrafish rapidly identifies genes essential for early vertebrate development. Nat Genet 2002;31:135–40.

23. MacArthur CA, Shankar DB, Shackleford GM. Fgf-8, activated by proviral insertion, cooperates with the Wnt-1 transgene in murine mammary tumorigenesis. J Virol 1995;69:2501–7.

24. Valve EM, Tasanen MJ, Ruohola JK, Harkonen PL. Activation of Fgf8 in S115 mouse mammary tumor cells is associated with genomic integration of mouse mammary tumor virus. Biochem Biophys Res Commun 1998;250:805–8.

25. Theodorou V, Kimm MA, Boer M, et al. MMTV insertional mutagenesis identifies genes, gene families and pathways involved in mammary cancer. Nat Genet 2007;39:759–69.

26. Reifers F, Bohli H, Walsh EC, Crossley PH, Stainier DY, Brand M. Fgf8 is mutated in zebrafish acerebellar (ace) mutants and is required for maintenance of midbrain-hindbrain boundary development and somitogenesis. Development 1998;125:2381–95.

27. Heisenberg C-P, Brennan C, Wilson SW. Zebrafish aussichtmutant embryos exhibit widespread overexpression of ace (fgf8) and coincident defects in CNS development. Development 1999;126:2129–40.

28. Albertson RC, Yelick PC. Fgf8 haploinsufficiency results in distinct craniofacial defects in adult zebrafish. Dev Biol 2007;306:505–15.

29. Topp S, Stigloher C, Komisarczuk AZ, Adolf B, Becker TS, Bally-Cuif L. Fgf signaling in the zebrafish adult brain: association of Fgf activity with ventricular zones but not cell proliferation. J Comp Neurol 2008;510:422–39.

30. Ellingsen S, Laplante MA, Konig M, et al. Large-scale enhancer detection in the zebrafish genome. Development 2005;132:3799–811.

31. Kikuta H, Laplante M, Navratilova P, et al. Genomic regulatory blocks encompass multiple neighboring genes and maintain conserved synteny in vertebrates. Genome Res 2007;17:545–55.

32. Gaiano N, Allende M, Amsterdam A, Kawakami K, Hopkins N. Highly efficient germ-line transmission of proviral insertions in zebrafish. Proc Natl Acad Sci U S A 1996;93:7777–82.

33. Wang D, Jao LE, Zheng N, et al. Efficient genome-wide mutagenesis of zebrafish genes by retroviral insertions. Proc Natl Acad Sci U S A 2007;104:12428–33.

34. Inoue F, Nagayoshi S, Ota S, et al. Genomic organization, alternative splicing, and multiple regulatory regions of the zebrafish fgf8 gene. Dev Growth Differ 2006;48:447–62.

35. Beermann F, Kaloulis K, Hofmann D, Murisier F, Bucher P, Trumpp A. Identification of evolutionarily conserved regulatory elements in the mouse Fgf8 locus. Genesis 2006;44:1–6.

36. Sidow A, Bulotsky MS, Kerrebrock AW, et al. A novel member of the F-box/WD40 gene family, encoding dactylin, is disrupted in the mouse dactylaplasia mutant. Nat Genet 1999;23:104–7.

37. Kano H, Kurahashi H, Toda T. Genetically regulated epigenetic transcriptional activation of retrotransposon insertion confers mouse dactylaplasia phenotype. Proc Natl Acad Sci U S A 2007;104:19034–9.

38. de Mollerat XJ, Gurrieri F, Morgan CT, et al. A genomic rearrangement resulting in a tandem duplication is associated with split hand-split foot malformation 3 (SHFM3) at 10q24. Hum Mol Genet 2003;12:1959–71.

39. Lyle R, Radhakrishna U, Blouin JL, et al. Split-hand/split-foot malformation 3 (SHFM3) at 10q24, development of rapid diagnostic methods and gene expression from the region. Am J Med Genet A 2006;140:1384–95.

40. Ye W, Shimamura K, Rubenstein JLR, Hynes MA, Rosenthal A. FGF and Shh signals control dopaminergic and serotonergic cell fate in the anterior neural plate. Cell 1998;93:755–66.

41. Guo S, Brush J, Teraoka H, et al. Development of noradrenergic neurons in the zebrafish hindbrain requires BMP, FGF8, and the homeodomain protein soulless/Phox2a. Neuron 1999;24:555–66.

42. Nechiporuk A, Linbo T, Poss KD, Raible DW. Specification of epibranchial placodes in zebrafish. Development 2007;134:611–23.

43. Kawauchi S, Shou J, Santos R, et al. Fgf8 expression defines a morphogenetic center required for olfactory neurogenesis and nasal cavity development in the mouse. Development 2005;132:5211–23.

44. Wang C, Xia C, Bian W, et al. Cell aggregation-induced FGF8 elevation is essential for P19 cell neural differentiation. Mol Biol Cell 2006;17:3075–84.

45. Reimers D, López-Toledano MA, Mason I, et al. Developmental expression of fibroblast growth factor (FGF) receptors in neural stem cell progeny. Modulation of neuronal and glial lineages by basic FGF treatment. Neurol Res 2001;23:612–21.

46. Nissen RM, Yan J, Amsterdam A, Hopkins N, Burgess S. Zebrafish foxi one modulates cellular responses to Fgf signaling required for the integrity of ear and jaw patterning. Development 2003;130:2543–54.

47. Marsh SK, Bansal GS, Zammit C, et al. Increased expression of fibroblast growth factor 8 in human breast cancer. Oncogene 1999;18:1053–60.

48. Dorkin TJ, Robinson MC, Marsh C, Bjartell A, Neal DE, Leung HY. FGF8 over-expression in prostate cancer is associated with decreased patient survival and persists in androgen independent disease. Oncogene 1999;18:2755–61.

49. Mattila MM, Harkonen PL. Role of fibroblast growth factor 8 in growth and progression of hormonal cancer. Cytokine Growth Factor Rev 2007;18:257–66.

50. Hunter DJ, Kraft P, Jacobs KB, et al. A genome-wide association study identifies alleles in FGFR2 associated with risk of sporadic postmenopausal breast cancer. Nat Genet 2007;39:870–4.

51. Huijts PE, Vreeswijk MP, Kroeze-Jansema KH, et al. Clinical correlates of low-risk variants in FGFR2, TNRC9, MAP3K1, LSP1 and 8q24 in a Dutch cohort of incident breast cancer cases. Breast Cancer Res 2007;9:R78.

52. Zhong C, Saribekyan G, Liao CP, Cohen MB, Roy-Burman P. Cooperation between FGF8b overexpression and PTEN deficiency in prostate tumorigenesis. Cancer Res 2006;66:2188–94.

53. Moore JL, Aros M, Steudel KG, Cheng KC. Fixation and decalcification of adult zebrafish for histological, immunocytochemical, and genotypic analysis. BioTechniques 2002;32:300–4.

54. Amsterdam A, Hopkins N. Retroviral-mediated insertional mutagenesis in zebrafish. Methods Cell Biol 2004;77:3–30.

55. Danielian PS, Bender Kim CF, Caron AM, Vasile E, Bronson RT, Lees JA. E2f4 is required for normal development of the airway epithelium. Dev Biol 2007;305:564–76.